

1 **On the relationship between hydrogen saturation in the tropical Atlantic Ocean and**
2 **nitrogen fixation by the symbiotic diazotroph UCYN-A**

3
4 **R. M. Moore¹, I. Grefe², J. Zorz³, S. Shan¹, K.Thompson¹, J. Ratten³, J. LaRoche³**

5 ¹Department of Oceanography, Dalhousie University, Halifax, Canada

6 ²Now at Lancaster Environment Centre, Lancaster University, Lancaster, UK

7 ³Department of Biology, Dalhousie University, Halifax, Canada

8
9 Corresponding author: Robert Moore (robert.moore@dal.ca)

10
11 Key points: Hydrogen supersaturation widespread across a tropical N. Atlantic transect.

12 Saturations correlated with UCYN-A *nifH* abundance

13 High resolution H₂ measurements are capable of illustrating space and time scales
14 of UCYN-A diazotrophy

15
16
17
18 Headings: Abstract

19 1 Introduction

20 2 Methods

21 3 Physical Oceanographic Conditions

22 4 Hydrogen analysis

23 5 Filtered seawater sample collection and nucleic acid extraction

24 6 qPCR

25 7 Results

26 8 Discussion

27

28

29

30

31 **Abstract**

32 Dissolved hydrogen measurements were made at high resolution in surface waters along a
33 tropical north Atlantic transect between Guadeloupe and Cape Verde in 2015 (Meteor 116).
34 Parallel water samples acquired to assess the relative abundance of the *nifH* gene from several
35 types of diazotrophs, indicated that *Trichodesmium* and UCYN-A were dominant in this region.
36 We show that a high degree of correlation exists between the hydrogen saturations and UCYN-A
37 *nifH* abundance, and a weak correlation with *Trichodesmium*. The findings suggest that nitrogen
38 fixation by UCYN-A is a major contributor to hydrogen supersaturations in this region of the
39 ocean. The ratio of hydrogen released to nitrogen fixed has not been determined for this
40 symbiont, but the indications are that it may be high in comparison with the small number of
41 diazotrophs for which the ratio has been measured in laboratory cultures. We speculate that this
42 would be consistent with the diazotroph being an exosymbiont on its haptophyte host. Our high
43 resolution measurements of hydrogen concentrations are capable of illustrating the time and
44 space scales of inferred activity of diazotrophs in near real-time in a way that cannot be achieved
45 by biological sampling and rate measurements requiring incubations with $^{15}\text{N}_2$. Direct
46 measurement of high resolution spatial variability would be relatively challenging through
47 collection and analysis of biological samples by qPCR, and extremely challenging by ^{15}N -uptake
48 techniques, neither of which methods yields real-time data. Nonetheless, determination of
49 fixation rates still firmly depends on the established procedure of incubations in the presence of
50 $^{15}\text{N}_2$.

51 **1 Introduction**

52 It has long been known that nitrogen fixation, the critical process for maintaining a
53 source of combined nitrogen to biota, involves production of molecular hydrogen. Pioneering
54 work on the relationship between hydrogen concentrations and nitrogen fixation in the oceans
55 was reported in a series of papers by Herr (e.g. *Herr and Barger, 1978*) and Scranton (e.g.
56 *Scranton et al. 1982*). *Ogo et al. [2004]* propose that the H_2 is displaced from a dihydride-
57 activated reaction centre of the nitrogenase enzyme. While the stoichiometry of the Equation 1
58 indicates



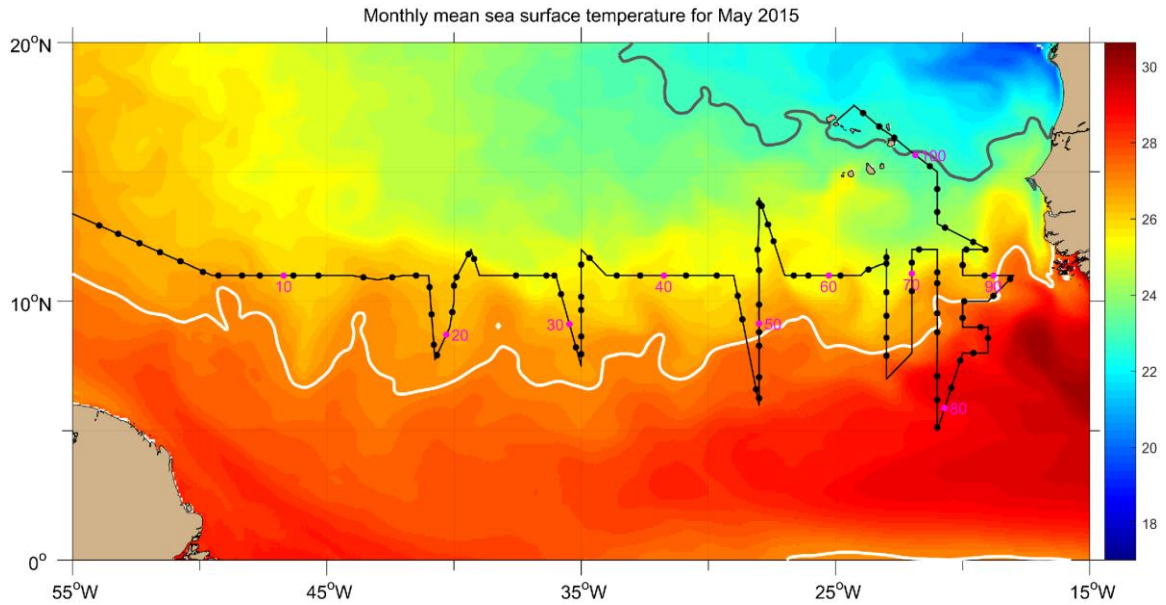
60 displacement of one hydrogen molecule for each N_2 reduced, the few laboratory studies made on
61 marine diazotrophs show highly variable net releases, with a value of 0.28 reported for
62 *Trichodesmium*, one order of magnitude less for *Cyanothece*, and two orders of magnitude less
63 for *Crocospaera* [*Wilson et al., 2010*]. The lower than stoichiometric releases are attributed to
64 recycling of hydrogen by its producer. We propose that diazotrophy in the oceans may
65 (depending on the extent to which the main diazotrophs release rather than recycle hydrogen)
66 lead to an easily measured supersaturation of hydrogen capable of acting as a general indicator of
67 nitrogen fixation. This is made possible by the fact that hydrogen concentrations in the
68 atmosphere are reasonably uniform in each hemisphere with mixing ratios of *ca.* 0.5 ppm in the
69 northern hemisphere, and 0.52 ppm in the southern [*Simmonds et al., 2000*]. These
70 concentrations reflect the balance of major sources of hydrogen, namely biomass burning and
71 photolytic oxidation of hydrocarbons such as methane and isoprene in the atmosphere [*Levy,*
72 *1972; Novelli et al., 1999*], and sinks – oxidation by OH in the atmosphere, and bacterial

73 consumption in soils which is weighted towards the northern hemisphere [Levy, 1972; Rhee et
74 al., 2005]. Coupled with the low aqueous solubility of hydrogen, the low atmospheric abundance
75 leads to a low and easily calculated equilibrium concentration in surface waters. Against this
76 background any net source of H₂ in nitrogen fixation should show as a significant supersaturation
77 [Moore et al., 2009]. Processes acting to diminish any saturation include loss to the atmosphere,
78 consumption by other microorganisms in the water column [Punshon et al., 2007; Barz et al.,
79 2010], and downward mixing.

80 Nitrogen fixation rates can be quantified using ¹⁵N₂ incubation methods and subsequent
81 isotope ratio mass-spectrometric analysis [Montoya et al., 1996]. This method, however, is
82 labour-intensive and unless attention is paid to complete equilibration of the tracer, prone to
83 errors such that nitrogen fixation by diazotrophs is underestimated [Großkopf et al., 2012; Mohr
84 et al., 2010], and batches of ¹⁵N₂ need to be checked for ¹⁵NH₃ contamination [Dabundo et al.,
85 2014]. Analysis of dissolved H₂ on the other hand can be carried out by a semi-automated system
86 at sea with measurements every 3.5 minutes [Moore et al., 2014]. While it cannot provide a
87 measure of nitrogen fixation rates, particularly because of the complexities introduced by
88 unquantified biological consumption rates, as well as the unknown degree of recycling by
89 diazotrophs themselves, it has been proposed as a near real-time indicator of active nitrogen
90 fixation [Moore et al., 2009] with the potential to survey large areas of the ocean for active
91 nitrogen fixation and to support ¹⁵N₂ incubation studies by identifying important areas for
92 accurate rate determinations. The objective of the work presented here is to further explore the
93 relationship between H₂ saturations and nitrogen fixation by diazotrophs, using qPCR to
94 enumerate several *nifH* phylotypes in DNA and RNA samples. The qPCR measurements of the
95 *nifH* phylotypes, expressed as *nifH* DNA copies L⁻¹ provided a measure of the distribution and
96 relative abundance of the major diazotrophs known to inhabit oceanic waters within this region
97 of the Tropical Atlantic. Although *nifH* RNA levels are indicative of active nitrogen fixation,
98 they are out of phase with protein synthesis, and therefore do not usually directly correlate with
99 nitrogenase [Church et al., 2005]. It should be noted that for logistical reasons during the cruise
100 described here direct measurements of nitrogen-fixation, for example by ¹⁵N₂ uptake, could not
101 be performed. In addition, any such incubation measurement that requires long incubation
102 periods (24-48 h in oligotrophic waters) cannot yield results that are congruent with the high
103 resolution H₂ data.

104 **2 Methods**

105 Dissolved H₂ concentrations were measured at 3.5 minute intervals in the surface ocean
106 during research cruise M116 on board RV Meteor (1st May-3rd June 2015, Pointe-à-Pitre,
107 Guadeloupe, to Mindelo, Cape Verde, Figure 1).



108

109 **Figure 1.** Cruise track and monthly mean sea surface temperature (SST) for May 2015. The
 110 month's average SST was calculated from the daily SST predictions from an operational forecast
 111 system (PSY4V3R1, see text for details). The ship track is shown by the black line, and dots
 112 denote positions of 103 discrete nucleic acid samples; sample numbers are indicated at intervals
 113 of 10. The 27°C isotherm is shown by the white contour, and 23°C by grey.

114 3 Physical Oceanographic Conditions

115 An overview of the prevailing physical oceanographic conditions of the study region was
 116 obtained from an operational global data-assimilative ocean 1/12° physics analysis and forecast
 117 system (PSY4V3R1). The PSY4V3R1 uses the NEMO 3.1 (Nucleus for European Models of the
 118 Ocean) modelling system with a horizontal resolution of 9 km at the equator and 50 levels in the
 119 vertical with 1m resolution near the surface. We focused on daily mean fields of sea level, sea
 120 surface temperature, salinity and current. To assess the reliability of model predictions of sea
 121 surface temperature and salinity we compared them with the corresponding observations made
 122 from the ship. The standard deviation of the differences was 0.39°C and 0.15 for temperature and
 123 salinity, respectively.

124 The general circulation in the shiptrack-covered equatorial region is briefly reviewed.
 125 Previous studies have shown that the zonal mean surface circulation, from 20°N towards the
 126 equator includes (1) the westward flowing North Equatorial Current (NEC), (2) the seasonal
 127 eastward flowing North Equatorial Countercurrent (NECC), and (3) the westward flowing
 128 Northern South Equatorial Current (NSEC, see Philander, 2001; Talley *et al.*, 2011). The NECC
 129 lies between 3°N and 10°N and begins to form at about 5°N in May, in response to a northward
 130 shift of the Intertropical Convergence Zone (ITCZ) associated with heavy rainfall. These features
 131 are evident in the mean surface circulation predicted by PSY4V3R1 for the study period. In
 132 addition, relatively low surface salinity was observed adjacent to the southernmost stations
 133 (locations of Samples #46 and #79 in Figure 1) in the ITCZ in May 2015 that, based on the
 134 atmospheric fields used to drive the ocean forecast system, was due to precipitation associated
 135 with the passage of an intense storm. Two coastal currents are also evident in the monthly mean
 136 SST field shown in Figure 1: the North Brazil Current and the Canary Current. The North Brazil

137 Current carries warm water of South Atlantic origin to the northwest along the coast of Brazil.
138 The Canary Current is associated with relatively cold upwelled water, and flows along the
139 African coast from north to south.

140 **4 Hydrogen analysis**

141 The analytical method is described in *Moore et al.* [2014]. In brief, water from the ship's
142 clean seawater supply was introduced by Tygon tubing to the bottom of a glass reservoir and
143 allowed to overflow. A peristaltic pump (REGLO Digital, Ismatec) supplied seawater from the
144 bottom of the reservoir to a bubble-segmented glass coil equilibrator [*Moore et al., 2014; Xie et*
145 *al., 2001*], with hydrocarbon-free air (Ultra Zero Air, Praxair) being used to provide the gas
146 bubbles in the equilibrator, as well as a carrier gas for the H₂ analyser. The gas phase was
147 separated from the water phase at the top end of the equilibrator and fed into a 1 mL sample loop
148 of a Peak Performer 1 Reducing Compound Photometer (PP1 RCP, Peak Laboratories, LLC). H₂
149 and CO were separated on a molecular sieve column and their concentrations were measured
150 using a heated mercuric oxide bed and UV absorption detector. The instrument's built-in
151 software was used to evaluate peak areas. H₂ measurements were corrected with measurements
152 of a low concentration gas standard (1.135 ppm) after every 20 seawater measurements.
153 Furthermore, equilibrator efficiency was monitored daily throughout the cruise using seawater
154 equilibrated with a 4.93 ppm H₂ standard (Praxair). The low concentration standard was prepared
155 by gravimetric dilution of the 4.93 ppm standard in zero air. Seawater concentrations of H₂ were
156 calculated using equilibrium solubilities described by *Wiesenburg and Guinasso* [1979].

157 Zinc anodes on the ship's hull can lead to H₂ contamination, while biofilms growing
158 inside the seawater plumbing can take up H₂ and lead to an underestimation of concentrations in
159 seawater. As the seawater intake was at the bow of the ship, contamination from anodes during
160 transit was highly unlikely; the plumbing was PVC and thus not a potential H₂ source. Therefore,
161 only data for ship's velocities above 6 knots were used for analysis. Another potential problem is
162 the accumulation of biofilms within seawater pipes. Bacteria forming those films can consume
163 H₂ [*Moore et al., 2009*], so the seawater pipes leading to the laboratory were cleaned with diluted
164 hypochlorite bleach (12%) before the cruise and again on 23 May 2015 as an originally planned
165 precaution against regrowth of biological films. To monitor for H₂ consumption within the
166 seawater pipes, water was collected from the thermosalinograph inlet, approximately 6 m
167 downstream of the bow inlet and compared with underway measurements. Underway and
168 discrete samples were usually within 0.2 nmol L⁻¹.

169 **5 Filtered seawater sample collection and nucleic acid extraction**

170 Water samples were collected for filtration and qPCR analysis, typically three times a
171 day during transit from the same laboratory seawater used for H₂ measurements, giving a total of
172 103 samples. Approximately 3L of seawater were collected in a low-density 4 L polyethylene
173 bottle. A 10 ml disposable pipette with an attached prefilter 160 µm mesh was connected to
174 Masterflex tubing and lowered into the sample collection bottle and the seawater sample was
175 filtered onto a 3 µm filter, followed by a 0.2 µm filter (both Isopore, Millipore) using a peristaltic
176 pump at 30 rpm (FH100 Peristaltic Variable Pump System, Thermo Scientific). The filtration
177 was stopped after 20 min to minimize degradation of RNA, and the exact filtration volume was
178 recorded. The 3 and 0.2 µm filters were placed in cryotubes and flash-frozen in liquid N₂.
179 Samples were stored at -80°C until analysis. We considered the sum of the two filters for all of

180 the measurements. The 160 μm mesh was used to prevent copepods and other large zooplankton
181 from overwhelming the microbial community signal with DNA from multicellular eukaryotic
182 organisms. The use of a pre-filter may have led to an underestimation of large *Trichodesmium*
183 filaments and colonies when present. However, the density of *Trichodesmium* colonies reported
184 in this region range from 0-2900 colonies m^{-3} and is on average at a density of less than 500
185 colonies m^{-3} : Singh *et al.* 2017), making it unlikely that they would have been present in a 3 L
186 water sample. Furthermore, the prefilter did not prevent the collection of the trichomes
187 (*Trichodesmium* filaments) as these were visually observed on the 3 μm filters in several areas
188 that are known habitat for *Trichodesmium*. Samples were extracted using the AllPrep DNA/RNA
189 Mini Kit (Qiagen) following manufacturer's instructions. RNA was transcribed to cDNA using
190 SuperScript III Reverse Transcriptase (Invitrogen) and PCR primers *nifH2* and *nifH3* (Zehr *et*
191 *al.*, 2003).

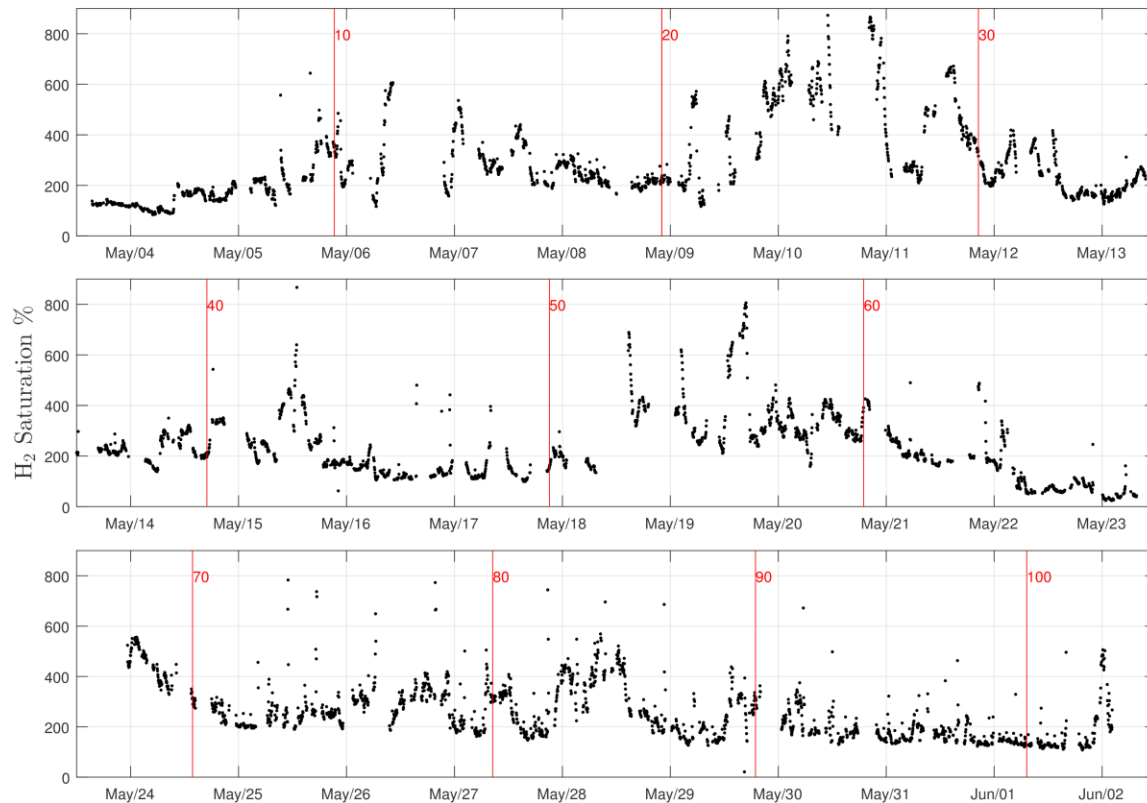
192 **6 qPCR**

193 Abundances of *nifH* gene or transcript copies per liter of seawater were estimated for
194 filamentous cyanobacteria (*Trichodesmium* and *Katagnymene* – hereafter referred to as simply
195 *Trichodesmium*), UCYN-A (*Candidatus Atelocyanobacterium thalassa*), UCYN-B
196 (*Crocospaera*), UCYN-C (*Cyanothece*), *Rhizosolenia* (*Richelia* symbionts, H1), *Hemiaulus*
197 (*Richelia* symbiont, H2), Cluster III and the γ -proteobacterial group Gamma A, using *nifH*-
198 phylotype specific primers and TaqMan probes and following the method described in Langlois
199 *et al.* (2008). Environmental DNA and cDNA samples were diluted 1:5 with qPCR water and 5
200 μL was added to the qPCR reaction. Samples were measured on a ViiA 7 Real-Time PCR
201 thermocycler (Applied Biosystems) and analysed using the manufacturer's software. The default
202 cycling program was used but the number of cycle was increased from 40 to 45. The Taqman
203 assays were calibrated using nucleotide standard specific for each *nifH* phylotypes as described
204 in Langlois *et al.*, [2008]. The qPCR results are reported in *nifH* copies L^{-1} for the various
205 phylotypes and this measurement cannot be extrapolated to cell counts and cannot be
206 intercompared quantitatively. In particular, it has been recently established that *Trichodesmium*
207 is polyploid, i.e. it contains several copies of the genome within a cell, making the *nifH* copies L^{-1}
208 1 much higher than the cell density (Sargent *et al.*, 2017). Therefore, the *nifH* assays are used
209 here only to assess the relative abundance within a specific phylotype. The various phylotypes
210 estimates cannot be added together to provide a total estimate of the total *nifH* copies L^{-1} as a
211 proxy for diazotroph abundance.

212 **7 Results**

213 Hydrogen saturations, shown in Figure 2, were highly variable but normally greater than
214 100% with a maximum of ca. 850%, and averaging around 250% (0.8 nmol L^{-1}). The only
215 significant period with substantial undersaturation was for 13 hours at 23°W, 9-11°N (May 22
216 2015) when saturation averaged 68%. No significant correlations were observed between
217 saturation and sea surface temperature, salinity, global radiation, windspeed (u , or u^2), or time of
218 day.

219



220
221

222 **Figure 2.** Hydrogen saturations along the cruise track plotted against time. The vertical lines
223 indicate the sampling time of stations marked in Figure 1.

224 As noted in the Method section, the absolute values of Taqman assays (*nifH* DNA copies
225 L^{-1}) for the various diazotrophs targeted here are neither representative of the cell density nor the
226 cellular biomass. The results were used in this study to assess the distribution and relative
227 abundance of each *nifH* phylotype in relation to the H_2 saturation. Throughout the transect,
228 *Trichodesmium* and UCYN-A were the most widely distributed diazotroph groups targeted by
229 the qPCR assays in the surface waters of the tropical Atlantic. The other *nifH* phylotypes (see
230 supplementary data) measured here were detected more sporadically throughout the transect and
231 showed no correlation with H_2 saturation and these groups are not further treated here. The
232 Taqman assays made with cDNA, representative of *nifH* transcript levels, also indicated that
233 *Trichodesmium* and UCYN-A were actively transcribing the *nifH* gene.

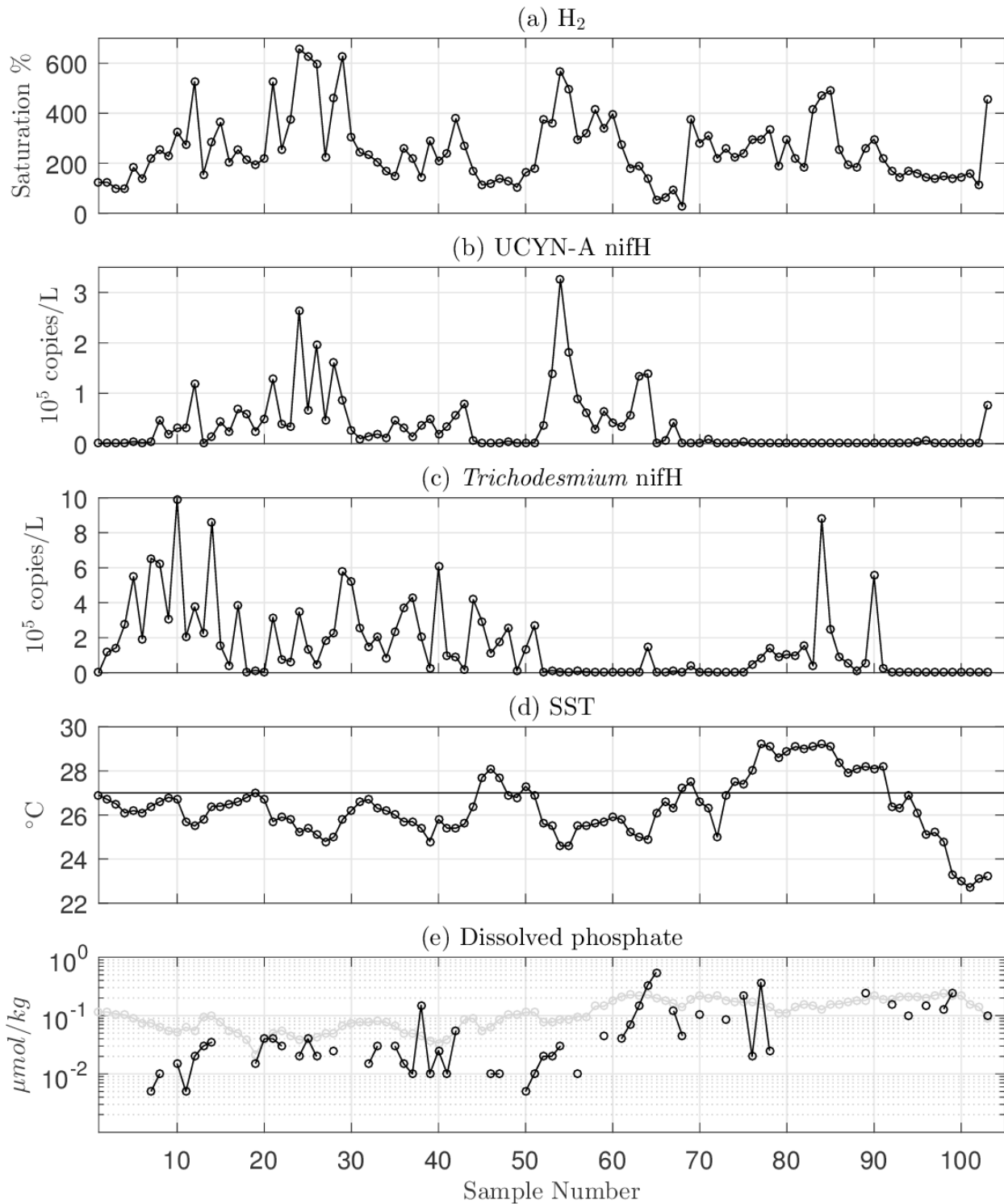
234

235 *Trichodesmium nifH* DNA concentrations (Figure 3) were generally high and variable to
236 the west of $28^\circ W$ (Samples 0-51), and mostly low to the east with the exception of some high
237 and variable values between 20 and $21^\circ W$ (Samples 84-90). UCYN-A was most abundant
238 between 48 and $23^\circ W$ (Samples 7-67, Figure 3) with the abundance showing clear signs of being
239 very low or undetected in surface waters warmer than about $27^\circ C$ (compare panels (b) and (d)).
240 These warmer waters also supported relatively high abundances of *Trichodesmium* (compare
241 panels (c) and (d)). A single high value of UCYN-A occurred in the coastal waters off Cape
242 Verde ($24^\circ W$; sample #103). A correspondence is apparent between samples having the highest
243 abundance of UCYN-A *nifH* copies and those with the highest H_2 saturations (Figure 3). This is
244 examined in more detail below.

245
246 A number of factors point to the existence of two groupings of samples, those west of
247 23°W (Samples 1-64), and those to the east. It is possible that it is related to an increase in
248 phosphate that occurs east of 23°W (Figure 3e; note the log scale of phosphate). Further
249 comments on differences between these regions are given in the Discussion. In the following
250 treatment we look first at the relationship between H₂ saturations and UCYN-A nifH abundance
251 in the sample western group (Samples 1-64) which cover most of the ocean basin.

252
253 Figure 4 suggests a linear relationship between the log of the H₂ saturation and the log of
254 UCYN-A abundance. In contrast there is no correlation between the H₂ saturation of these
255 samples and their abundance of *Trichodesmium* (Figure 5). However, the same figure shows that
256 if we select just those samples having UCYN-A abundances in the lowest one third of the entire
257 group, then some correlation emerges. It appears that the influence of *Trichodesmium* on H₂
258 saturation is overwhelmed by the influence of UCYN-A.

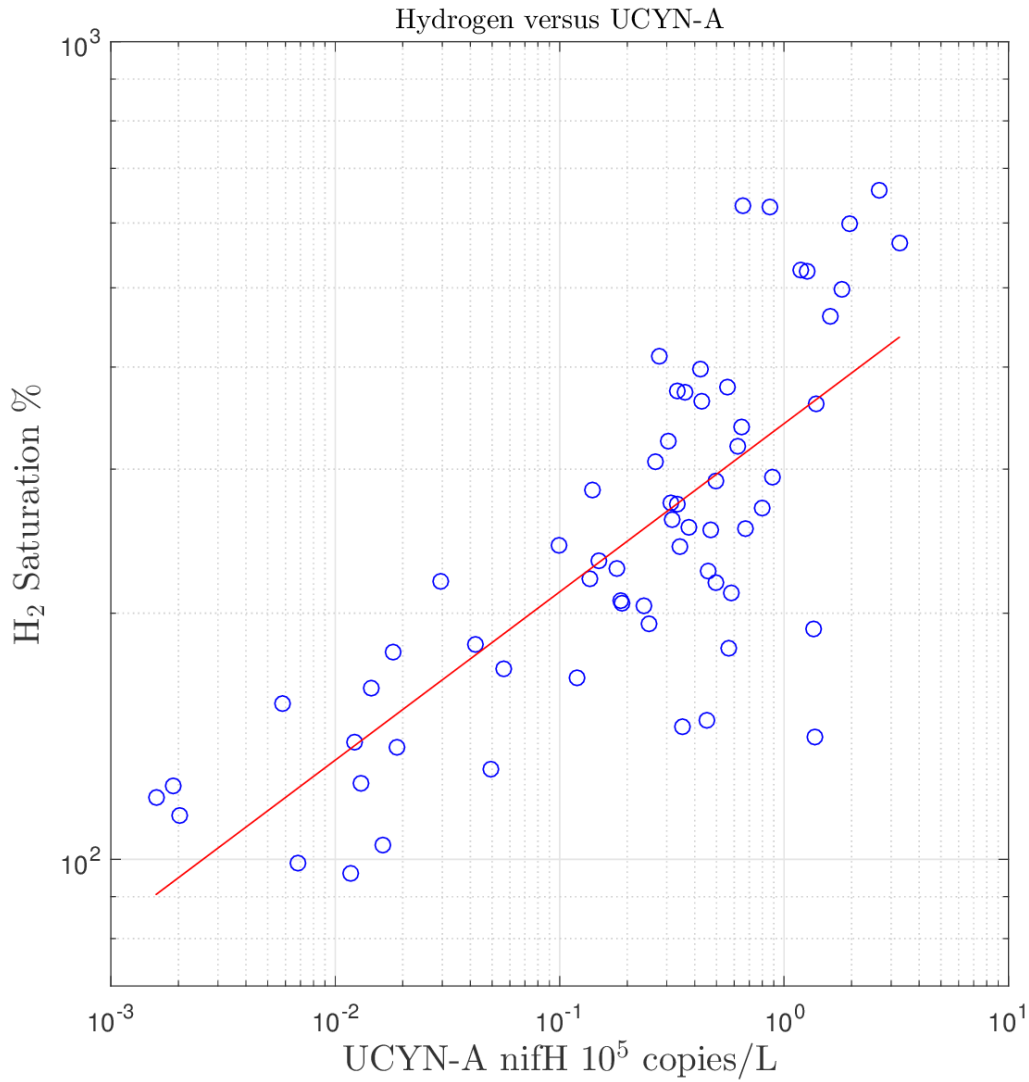
259 Using the relationship derived from Figure 4 a prediction (Figure 6) can be made for H₂
260 saturations based solely on UCYN-A abundance in this western zone of the cruise track.
261 Inspection of this plot suggests the predictive capability of a single variable, the abundance of a
262 single species of diazotroph, is remarkable, particularly in view of the fact that a realistic model
263 of hydrogen concentration would demand inclusion of loss to the atmosphere and microbial
264 consumption, the rates of which are unknown and presumably strongly dependent on the
265 composition of the local microbial community which itself may be affected by the hydrogen
266 concentration.
267



268
 269
 270
 271
 272
 273
 274

Figure 3. (a) Hydrogen saturations (average of 3 continuous measurements over the time of discrete water sample collection), (b) UCYN-A abundances, (c) *Trichodesmium* abundances, and (d) SST for discrete samples collected along the cruise track where horizontal line denotes T=27°C, the temperature maximum for UCYN-A; (e) measured dissolved phosphate

275 concentration (black circles) and mean surface phosphate based on interpolating the monthly
276 mean World Ocean Atlas 2013 version 2 climatology (Garcia *et al.*, 2014) for May to the ship
277 track (grey line). Refer to Fig.1 for exact sample locations.
278



279

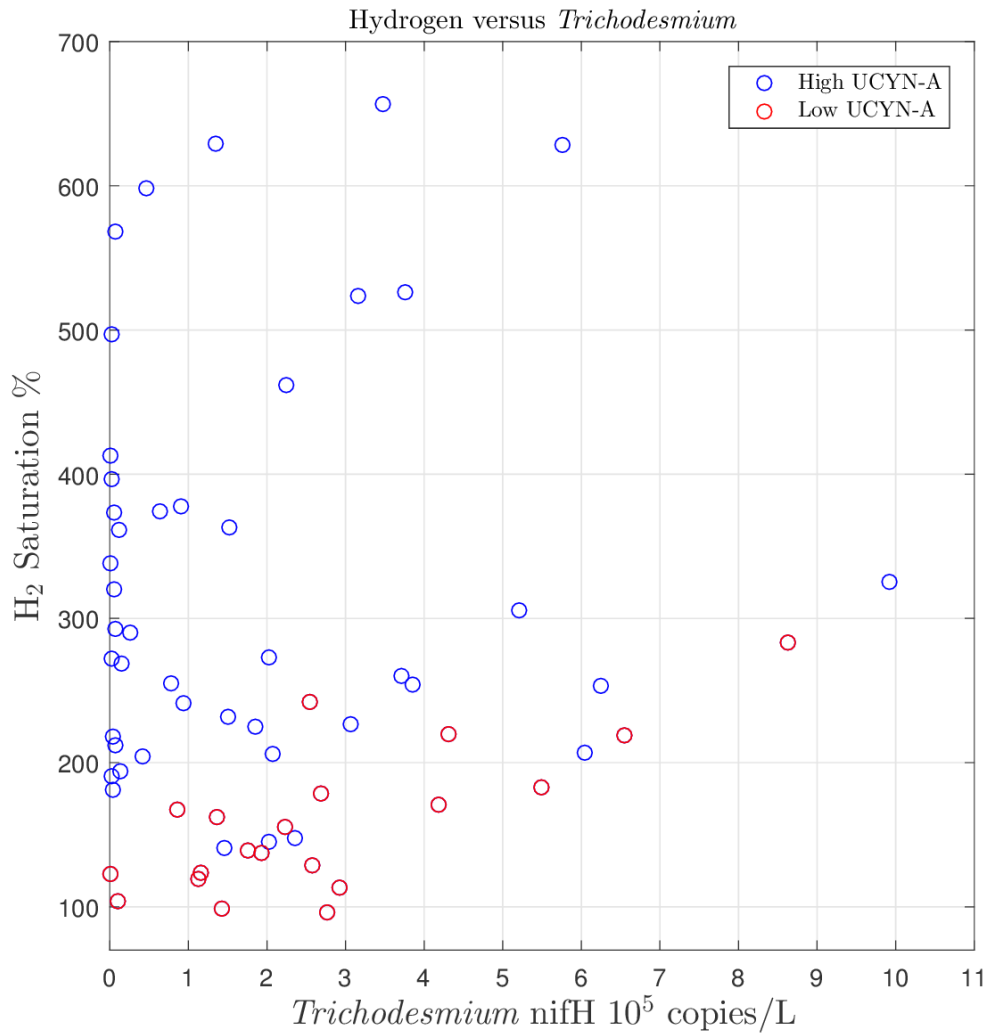
280

281

282 | **Figure 4.** Log-log plot of H_2 saturation against UCYN-A *nifH* copy abundance for Samples 1 to
283 64 inclusive. The red line shows the linear regression of $\log_e(H_2)$ on $\log_e(UCYN-A)$. The
284 intercept, slope and coefficient of determination were estimated to be 5.83 ± 0.10 , 0.206 ± 0.030
285 and $R^2 = 0.588 \pm 0.102$. The standard errors were estimated using the circular bootstrap with
286 blocking to allow for serial correlation of $\log_e(H_2)$ on $\log_e(UCYN-A)$. A block length of 8 was
287 selected based on simulation studies using a bivariate AR(1) process matched to the
288 observations.

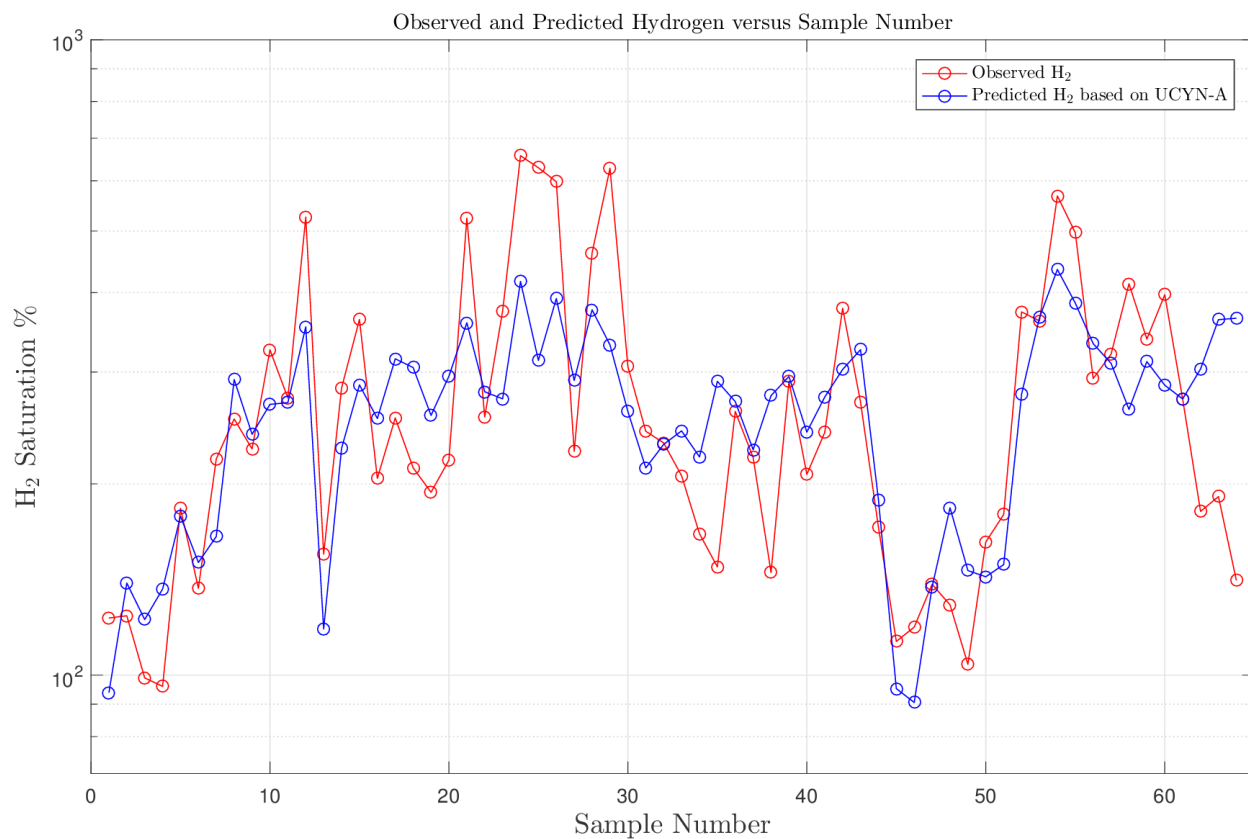
289

290



291
 292
 293
 294
 295

Figure 5. H₂ saturation plotted against *Trichodesmium nifH* gene abundance for 64 western samples; in red are the samples with low UCYN-A abundance (“low” defined in text).



296
297
298
299

Figure 6. H₂ saturation plotted (log scale) against sample number; red symbols represent observations, and blue represent predicted saturations based on UCYN-A *nifH* copy abundance.

300 **8 Discussion**

301 Hydrogen supersaturation in ocean surface waters has been reported in many publications
302 [e.g. *Herr and Barger, 1978; Scranton et al. 1982; Moore et al., 2009, 2014*], but in early work
303 there was much uncertainty about the sources, and it was recognised that contamination,
304 particularly from corroding metal, was difficult to avoid [*Scranton et al., 1982*]. It was
305 recognised that nitrogen fixation and photochemistry were potential sources in surface waters
306 [*Scranton 1983, 1984; Herr et al., 1984*]. As the current work focuses on surface waters we will
307 not discuss hydrogen production in anoxic environments, nor hydrothermal sources. *Punshon*
308 *and Moore* [2008a] have shown that while photochemical production is a large source in highly
309 coloured terrestrial waters, and possibly a source in coastal waters influenced by terrestrial
310 runoff, it is not expected to be significant in offshore ocean waters.

311 In the same way that nitrogen fixation studies have, over a long period, focussed on the
312 highly visible colonial species, *Trichodesmium*, so too has this species been the subject of studies
313 and discussion of its contributions to hydrogen supersaturation. There have been reports
314 supporting the notion that it produces hydrogen both in field studies [*Scranton 1984; Scranton et*
315 *al., 1987*], and laboratory studies [*Wilson et al., 2010; Punshon and Moore, 2008b*]. Indeed, with
316 so few quantifications of release ratios of H₂ to N₂ consumption, as well as very incomplete
317 knowledge of the extent and variety of different marine diazotrophs, it has been natural to link
318 hydrogen supersaturation to *Trichodesmium* activity or abundance. However, *Scranton et al.*

319 [1982] commented that in the surface waters of the Mediterranean “and probably elsewhere”,
320 organisms existing in oxygenated waters other than *Trichodesmium* (then *Oscillatoria*) must be
321 producing hydrogen.

322

323 UCYN-A (*Athelocyanobacterium thalassa*) has in recent years been recognised as a
324 potentially important contributor to marine nitrogen fixation [Zehr *et al.*, 2008; Krupke *et al.*
325 2013; Martinez-Perez *et al.*, 2016], and the current work reveals that it plays a major role in
326 supporting hydrogen supersaturation in the Equatorial Atlantic. The cyanobacterium UCYN-A,
327 lacking the photosystem II and the ability to fix carbon, is dependent on a photosynthetic host
328 that is a haptophyte [Thompson *et al.*, 2012]. The absence of oxygen production by this
329 symbiotic diazotroph might facilitate its ability to fix nitrogen [Bothe *et al.*, 2010]. The strong
330 correlation shown here between hydrogen saturation and UCYN-A abundance does not itself
331 prove causality, but since we know from Equation 1 that nitrogen fixation yields hydrogen, and
332 since a number of laboratory and field studies provide evidence for this, at least in the case of
333 *Trichodesmium*, we can deduce that nitrogen fixation by UCYN-A is a major, and probably the
334 primary, source of hydrogen saturation in our study. Martinez-Perez *et al.* [2016] report that
335 UCYN-A and its hosts have growth rates five to ten times higher than *Trichodesmium* and that
336 this leads to the conclusion that its contribution to nitrogen fixation is proportionately higher than
337 its cell abundances alone would suggest, those abundances being controlled by active grazing.
338 Stoichiometrically, hydrogen release follows the rate of nitrogen fixation, so the hydrogen signal
339 is not diminished by the grazing that checks the cell abundance. However, we have no
340 information on the rates at which hydrogen is being consumed by bacteria, nor do we know the
341 extent to which the symbionts themselves might recycle hydrogen. It may be quite significant
342 that there is evidence for UCYN-A being an exosymbiont [Martinez-Perez *et al.*, 2016], as
343 hydrogen that it must produce may be released directly to the environment, as opposed to being
344 channelled to (or through) its host as in the case of endosymbiotic associations like *Richelia-*
345 *Hemiaulus*.

346 In support of the strong correlation that we observed between H₂ supersaturation and
347 UCYN-A, we note that the spatial separation between O₂ evolution in the host and the symbiotic
348 diazotrophs might provide favourable conditions for diazotrophy and the associated H₂
349 production by the nitrogenase enzyme. In other cyanobacterial diazotrophs, the deactivation of
350 PSII (Bayro-kaiser and Nelson, 2016) and/or the diel cycle segregation of photosynthesis and
351 nitrogen fixation between light and dark periods (Bandyopadhyay *et al.* 2013) may lead to high
352 rates of H₂ production under aerobic conditions, by deriving the required energy for nitrogen
353 fixation from glycogen pools, either provided as an additional organic carbon source or acquired
354 through photosynthesis during the day. In the symbiotic UCYN-A, photosynthetically-derived
355 organic carbon from the host is transferred to the symbiont and likely fuels nitrogen fixation
356 (Martinez-Perez *et al.*, 2016). Additionally, the symbiont has the ability to carry out ATP
357 synthesis from sunlight through PSI driven cyclic electron flow (Zehr *et al.* 2016;
358 Bandyopadhyay *et al.*, 2010, 2011; Martinez-Perez *et al.*, 2016).

359 Diel cycling between nitrogen fixation (at night) and photosynthesis (during the day) is
360 common in unicellular cyanobacteria, but in cyanobacteria that have spatial separation of these
361 two processes, as for heterocystous cyanobacteria, the temporal segregation of nitrogen fixation
362 and photosynthesis is not observed. Except for the fact that we now know that the UCYN-A is a

363 symbiont on a haptophyte (Thompson *et al.* 2012 and Martinez-Perez *et al.* 2016), its lifestyle is
364 practically unknown because there is no cultured isolate of the symbiont and its host. Therefore,
365 the mechanism by which the symbiont's nitrogenase is protected from oxidative damage by the
366 host is currently unknown.

367 The reason for the existence of many samples to the east of 23°W that contain low or
368 zero abundances of *Trichodesmium* and UCYN-A is unknown, except that many of the samples
369 are from waters warmer than 27°C (Figure 1) and this appears to be outside the range for UCYN-
370 A. Preliminary analysis of *nifH* sequences obtained by high throughput sequencing also
371 suggest that another clade of UCYN-A and an alphaproteobacterial diazotroph dominated the
372 diazotrophic community east of 23°W (Jenni-Marie Ratten, Julie LaRoche, personal
373 communication), and were not targeted by the qPCR assays used in this study.

374 Our data show that surface waters can be substantially supersaturated even when UCYN-
375 A and *Trichodesmium* have low abundance. We can speculate on reasons for this: first, the
376 supersaturation might be accounted for by small contributions from several different diazotrophs,
377 including ones that are present at relatively low abundances; second, there may be active
378 diazotrophs other than those targeted by our work; and third, though unlikely, the hydrogen
379 signal sometimes dissipates more slowly than the responsible diazotroph(s).

380 The strong correlation found in this study leads us to propose that UCYN-A has a
381 significant value for the ratio, H₂ release/N₂ fixed, almost certainly higher than the values
382 reported for the unicellular cyanobacteria *Cyanothece* and *Crocospaera* (only 0.05 and 0.004
383 mol of H₂ per mol N₂ fixed), and probably higher than the value (0.28) for *Trichodesmium*
384 [Wilson *et al.*, 2010]. It would not be surprising if hydrogen release rates from a very small
385 number of laboratory studies with cultures differ from what occurs in the oceanic environment.

386 The weak relationship found in this study between hydrogen saturation and
387 *Trichodesmium* abundance, at least in the presence of significant abundance of UCYN-A, may
388 suggest that hydrogen saturations reported in the Pacific [Moore *et al.*, 2009] and Atlantic
389 [Moore *et al.*, 2012] are indicative of widespread nitrogen fixation by UCYN-A. One question
390 among many yet to be addressed on biological consumption of hydrogen is whether an organism
391 like *Trichodesmium* that is reported to recycle the greater part of the hydrogen it produces would,
392 in waters enriched in the gas from other sources, become a net consumer.

393 This work in the tropical Atlantic shows for the first time that hydrogen saturations in
394 surface waters can be related to the abundance of UCYN-A (and by inference its diazotrophic
395 activity). Our high resolution measurements of hydrogen (Figure 2) are capable of illustrating the
396 space and time scales of diazotrophy, in this instance apparently attributable to UCYN-A
397 activity. Direct measurement of such variability would be relatively challenging through
398 collection and analysis of biological samples by qPCR, and extremely challenging by ¹⁵N-uptake
399 techniques, neither of which methods yields real-time data. Nonetheless, rigorous determination
400 of nitrogen fixation rates depends on the established procedure of incubations in the presence of
401 ¹⁵N₂.

402 **Acknowledgements**

404 The authors acknowledge the support of the following: NSERC (RMM); the Canadian Research
405 Chairs Programme and Canada Fund for Innovation (JLR); the German Research Foundation,

406 DFG and Drs. Toste Tanhua and Martin Visbeck, Chief Scientist for the provision of ship time.
407 The cruise was organized by the Deutsche Forschungsgemeinschaft as part of the
408 Sonderforschungsbereich 754 “Climate-Biogeochemistry Interactions in the Tropical Ocean”.
409 The operational global data-assimilative ocean physics analysis and forecast
410 (GLOBAL_ANALYSIS_FORECAST_PHY_001_024, PSY4V3R1) output was downloaded
411 from <http://marine.copernicus.eu>. The authors acknowledge the constructive comments of three
412 reviewers.

413

414 **References**

415 Bandyopadhyay, A. et al. “Novel Metabolic Attributes of the Genus *Cyanothece*, Comparing a
416 Group of Unicellular Nitrogen-Fixing Cyanobacteria.” *mBio* 2.5 (2011): e00214-11 –e00214-11.

417

418 Bandyopadhyay, A. et al. “High Rates of Photobiological H₂ Production by a Cyanobacterium
419 under Aerobic Conditions.” *Nature communications* (2010): DOI: 10.1038/ncomms1139.

420

421 Bandyopadhyay, A. et al. (2013) Variations in the Rhythms of Respiration and Nitrogen
422 Fixation in Members of the Unicellular Diazotrophic Cyanobacterial Genus *Cyanothece*. *Plant*
423 *Physiology*, 161, 1334.

424 Barz, M., C. Beimgraben, T. Staller, F. Germer, F. Opitz, C. Marquardt, C. Schwarz, K.
425 Gutekunst, K.H. Vanselow, R. Schmitz, J. LaRoche, R. Schulz, and J. Appel (2010), Distribution
426 analysis of hydrogenases in surface waters of marine and freshwater environments, *PLoS One*,
427 5(11), e13846, doi:10.1371/journal.pone.0013846.

428 Bayro-kaiser V. and N. Nelson. “Temperature-Sensitive PSII: A Novel Approach for Sustained
429 Photosynthetic Hydrogen Production.” *Photosynthesis Research* 130.1 (2016): 113-121.

430 Bothe, H., H.J. Tripp and J.P. Zehr (2010), Unicellular cyanobacteria with a new mode of life:
431 the lack of photosynthetic oxygen evolution allows nitrogen fixation to proceed. *Archives*
432 *Microbiol.* 192, 783-790.

433 Church, M.J., et al. (2005), Temporal patterns of nitrogenase gene (*nifH*) expression in the
434 oligotrophic North Pacific Ocean, *Appl. Environ. Microb.*, 71(9), 5362-5370.

435 Dabundo, R, M.F. Lehmann, L. Treibergs, C.R. Tobias, M.A. Altabet, *et al.* (2014), The
436 contamination of commercial ¹⁵N₂ gas stocks with 15 N-labeled nitrate and ammonium and
437 consequences for nitrogen fixation measurements. *PLoS ONE* 9(10): e110335.
438 doi:10.1371/journal.pone.0110335.

439 Garcia, H. E., R. A. Locarnini, T. P. Boyer, J. I. Antonov, O.K. Baranova, M.M. Zweng, J.R.
440 Reagan, D.R. Johnson, 2014. *World Ocean Atlas 2013, Volume 4: Dissolved Inorganic Nutrients*
441 (phosphate, nitrate, silicate). S. Levitus, Ed., A. Mishonov Technical Ed.; NOAA Atlas NESDIS
442 76, 25 pp.

443 Großkopf, T. *et al.* (2012), Doubling of marine dinitrogen-fixation rates based on direct

444 measurements. *Nature* 488, 361-364, doi:10.1038/nature11338.

445 Herr, F.L., W.R. Barger (1978), Molecular hydrogen in the near surface atmosphere and
446 dissolved in waters of the tropical North Atlantic. *J. Geophys. Res.* 83, 6199-6205.

447 Herr, F.L., E.C. Frank, G.M. Leone, M.C. Kennicutt (1984), Diurnal variability of dissolved
448 molecular hydrogen in the tropical South Atlantic Ocean. *Deep-Sea Res.* 31, 13-20.

449 Krupke, A. et al. (2013), In situ identification and N₂ and C fixation rates of uncultivated
450 cyanobacteria populations. *Syst. Appl. Microbiol.*, 36 (2013) 259– 271.

451 Langlois, R.J., D. Hümmer, and J. LaRoche (2008), Abundances and distributions of the
452 dominant nifH phylotypes in the Northern Atlantic Ocean., *Appl. Environ. Microb.*, 74(6), 1922–
453 31, doi:10.1128/AEM.01720-07.

454 Levy, H. (1972), Photochemistry of the troposphere. *Planet. Space Sci.*, 20, 919-935.

455 Martinez-Perez et al., (2016), The small unicellular diazotrophic symbiont, UCYN-A, is a key
456 player in the marine nitrogen cycle, *Nat. Microbiol.*, DOI: 10.1038/NMICROBIOL.2016.163

457

458 Mohr, W. et al. 2010 Methodological Underestimation of Oceanic Nitrogen Fixation Rates. *PLoS*
459 *ONE* 5(9):e12583.

460 Moore, R.M., S. Punshon, C. Mahaffey, and D.M. Karl (2009), The relationship between
461 dissolved hydrogen and nitrogen fixation in ocean waters. *Deep-Sea Res. I*, 56, 1449-1458.

462 Moore, R. M., M. Kienast, M. Fraser, J.J. Cullen, C. Deutsch, S. Dutkiewicz, M.J. Follows and
463 C.J. Somes (2014), Extensive hydrogen supersaturations in the western South Atlantic Ocean
464 suggest substantial underestimation of nitrogen fixation, *J. Geophys. Res. Ocean.*, 119(7), 4340–
465 4350, doi:10.1002/2014JC010017.

466 Montoya, J.P., M. Voss, P. Kaehler, D.G. Capone (1996), A simple, high-precision, high-
467 sensitivity tracer assay for N₂ fixation, *Appl. Environ. Microb.*, 62, 986-993.

468 Novelli, P. C. et al. (1999), Molecular hydrogen in the troposphere: global distribution and
469 budget. *J. Geophys. Res.*, 104, 30427-30444.

470 Ogo, S., B. Kure, H. Nakai, Y. Watanabe, and S. Fukuzumi (2004), Why do nitrogenases waste
471 electrons by evolving dihydrogen? *Appl. Organomet. Chem.*, 18: 589–594,
472 DOI:10.1002/aoc.744.

473 Philander, S.G. (2001), Atlantic Ocean equatorial currents, In *Encyclopedia of ocean sciences*,
474 edited by John H. Steele, Academic Press, Oxford, pp 188-191, ISBN 9780122274305,
475 <http://dx.doi.org/10.1006/rwos.2001.0361>.
476 (<http://www.sciencedirect.com/science/article/pii/B012227430X003615>).

477 Punshon, S., R.M. Moore, and H. Xie (2007), Net loss rates and distribution of molecular
478 hydrogen in mid-latitude coastal waters. *Mar. Chem.*, 105, 129-139.

479 Punshon, S. and R.M. Moore (2008a), Photochemical production of molecular hydrogen in lake
480 water and coastal seawater. *Mar. Chem.*, 108, 215-220.

481 Punshon, S. and R.M. Moore (2008b), Aerobic hydrogen production and dinitrogen fixation in
482 the marine cyanobacterium *Trichodesmium erythraeum* IMS 101. *Limnol. Oceanogr.*, 53, 2749-
483 2753.

484 Rhee, T. S., C.A.M. Brenninkmeijer and T. Röckmann (2005), The overwhelming role of soils in
485 the global atmospheric hydrogen cycle, *Atmos. Chem. Phys. Discuss.*, 5, pp.11215–11248,
486 doi:10.5194/acpd-5-11215-2005.

487 Sargent, E.C., et al. (2016), Evidence for polyploidy in the globally important diazotroph
488 *Trichodesmium*. *FEMS Microbiol. Lett.*, 363(21), p.fnw244.

489 Scranton, M.I. (1983), The role of the cyanobacterium *Oscillatoria* (*Trichodesmium*) *thiebautii* in
490 the marine hydrogen cycle. *Mar. Ecol. Prog. Ser.* 11, 79-87.

491 Scranton, M.I. (1984), Hydrogen cycling in the waters near Bermuda: the role of the nitrogen
492 fixer, *Oscillatoria thiebautii*. *Deep-Sea Res.* 31, 133–143.

493 Scranton, M.I., M.M. Jones, and F.L. Herr (1982), Distribution and variability of dissolved
494 hydrogen in the Mediterranean Sea, *J. Mar. Res.*, 40: 873-891.

495 Scranton, M.I., P.C. Novelli, A. Michaels, S.G. Horrigan, and E.J. Carpenter (1987), Hydrogen
496 production and nitrogen fixation by *Oscillatoria thiebautii* during in situ incubations *Limnol.*
497 *Oceanogr.* 32, 998-1006

498 Simmonds, P.G. *et al.* (2000), Continuous high-frequency observations of hydrogen at the Mace
499 Head baseline atmospheric monitoring station over the 1994-1998 period. *J. Geophys. Res.*, 105:
500 12105-12121

501

502 Singh, A., L. T. Bach, T. Fischer, H. Hauss, R. Kiko, A. J. Paul, P. Stange, P. Vandromme, and
503 U. Riebesell (2017), Niche construction by non-diazotrophs for N₂ fixers in the eastern tropical
504 North Atlantic Ocean, *Geophys. Res. Lett.*, 44, 6904–6913, doi:10.1002/2017GL074218

505 Talley L. D., G.L. Pickard W.J. Emery, and J.H. Swift (2011), Introduction to descriptive
506 physical oceanography. Academic Press, Boston. 471 pp.

507 Thompson, A.W. *et al.* (2012), Unicellular cyanobacterium symbiotic with a single-celled
508 eukaryotic alga, *Science* 337, 1546; DOI: 10.1126/science.1222700.

509 Wiesenburg, D.A. and N.L. Guinasso (1979), Equilibrium solubilities of methane, carbon
510 monoxide and hydrogen in water and seawater, *J. Chem. Eng. Data*, 24, 356–360.

511 Wilson, S.T., R.A. Foster, J.P. Zehr, and D.M. Karl (2010), Hydrogen production by
512 *Trichodesmium erythraeum* Cyanothece sp. and *Crocospaera watsonii*. *Aquat. Microbiol. Ecol.*,
513 59, 197–206, doi: 10.3354/ame01407.

514 Xie, H., O.C. Zafiriou, W. Wang, and C.D. Taylor (2001), A simple automated continuous-flow-
515 equilibration method for measuring carbon monoxide in seawater, *Environ. Sci. Technol.*, 35 (7),
516 1475-1480• DOI: 10.1021/es001656v

517 Zehr, J.P., L.L. Crumbliss, M.J. Church, E.O. Omoregie, and B.D. Jenkins (2003), Nitrogenase
518 genes in PCR and RT-PCR reagents: Implications for studies of diversity of functional genes,
519 *Biotechniques*, 35(5), 996–1005.

520 Zehr et al. (2008), Globally distributed uncultivated oceanic N₂-fixing cyanobacteria lack
521 oxygenic photosystem II. *Science* 322, 1110-1112.

522 Zehr, J. P. et al. “Unusual Marine Unicellular Symbiosis with the Nitrogen-Fixing
523 *Cyanobacterium* UCYN-A.” *Nature Microbiology* 2.1 (2016): 16214.

Figure 1.

Monthly mean sea surface temperature for May 2015

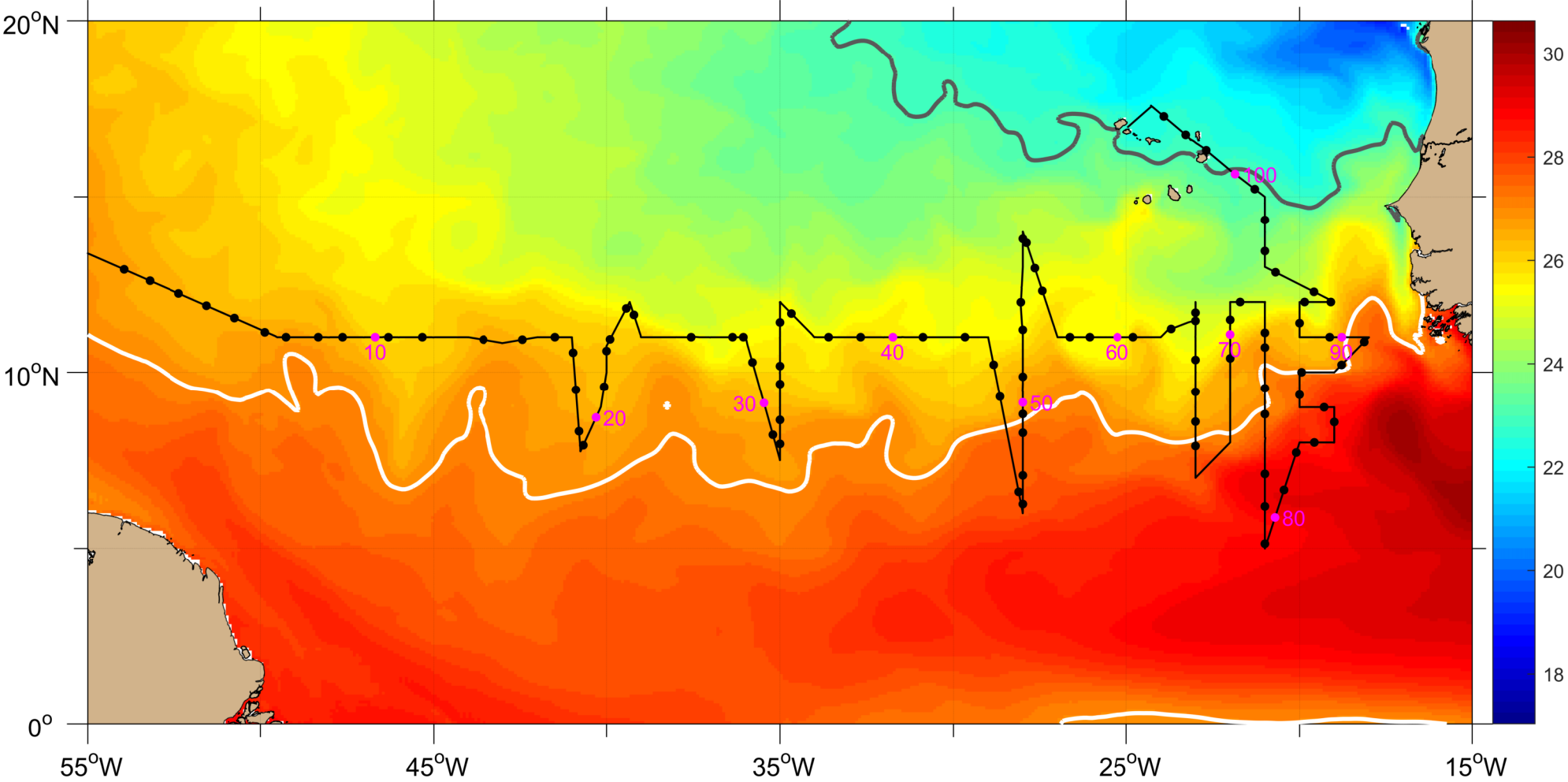


Figure 2.

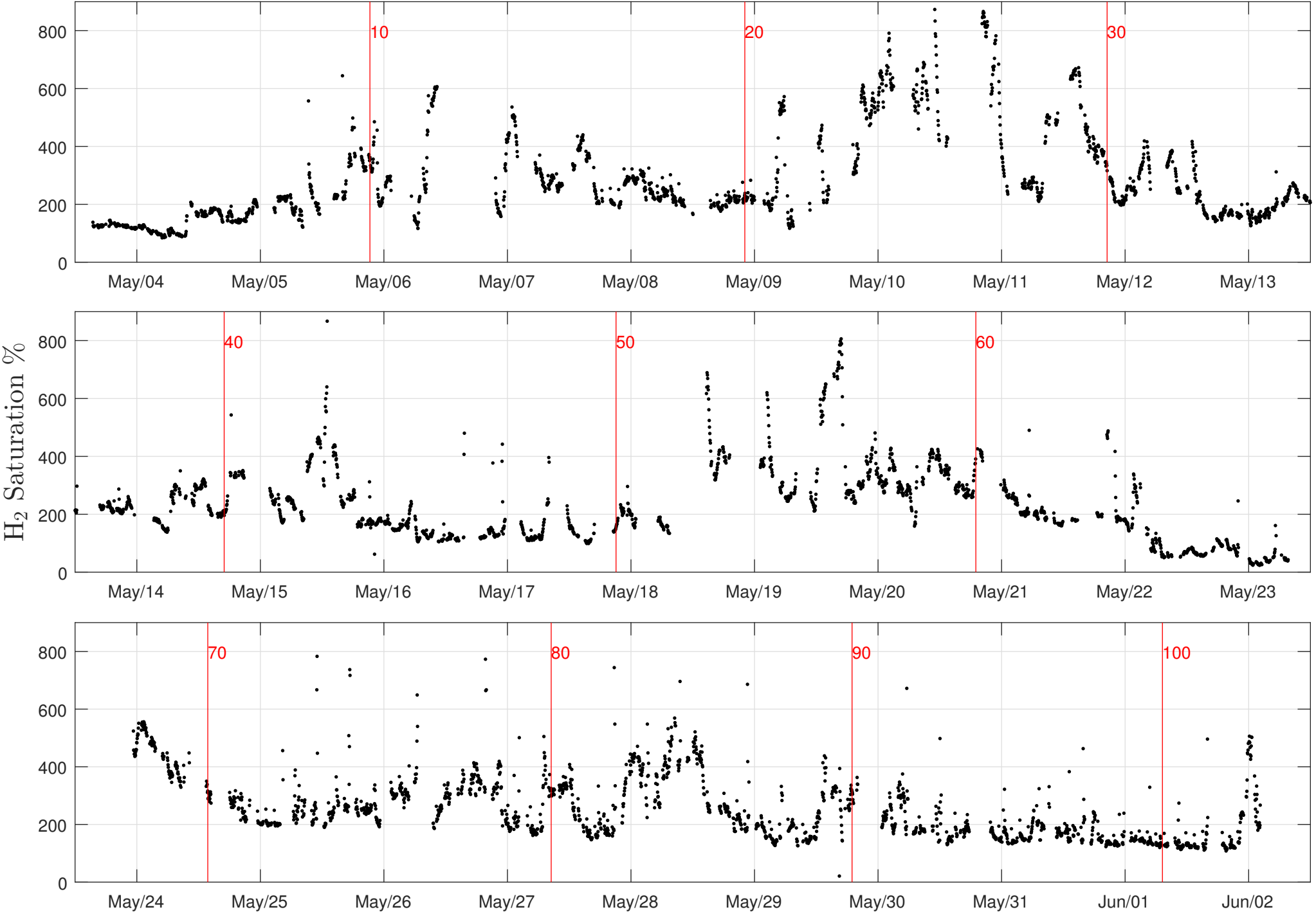


Figure 3.

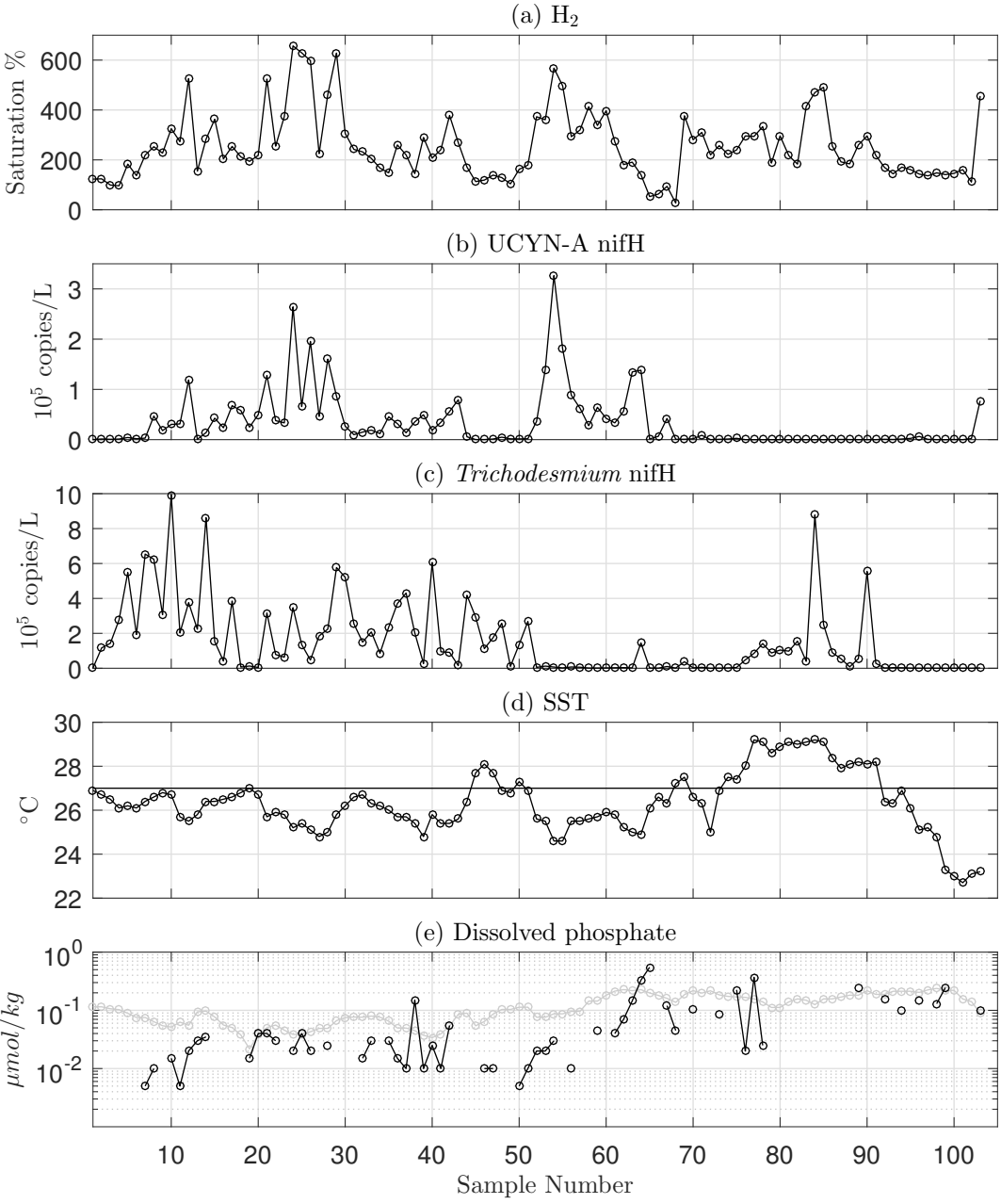


Figure 4.

Hydrogen versus UCYN-A

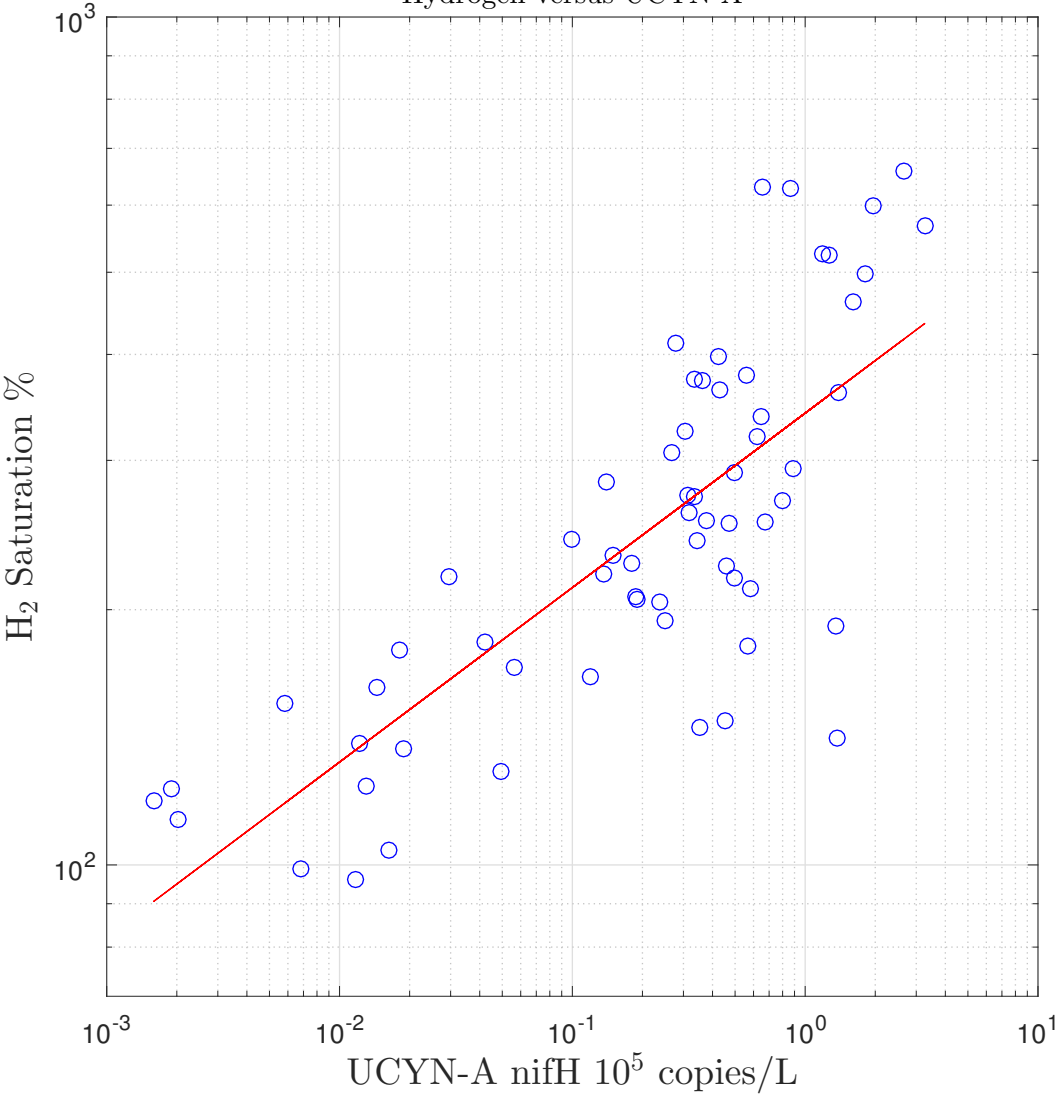


Figure 5.

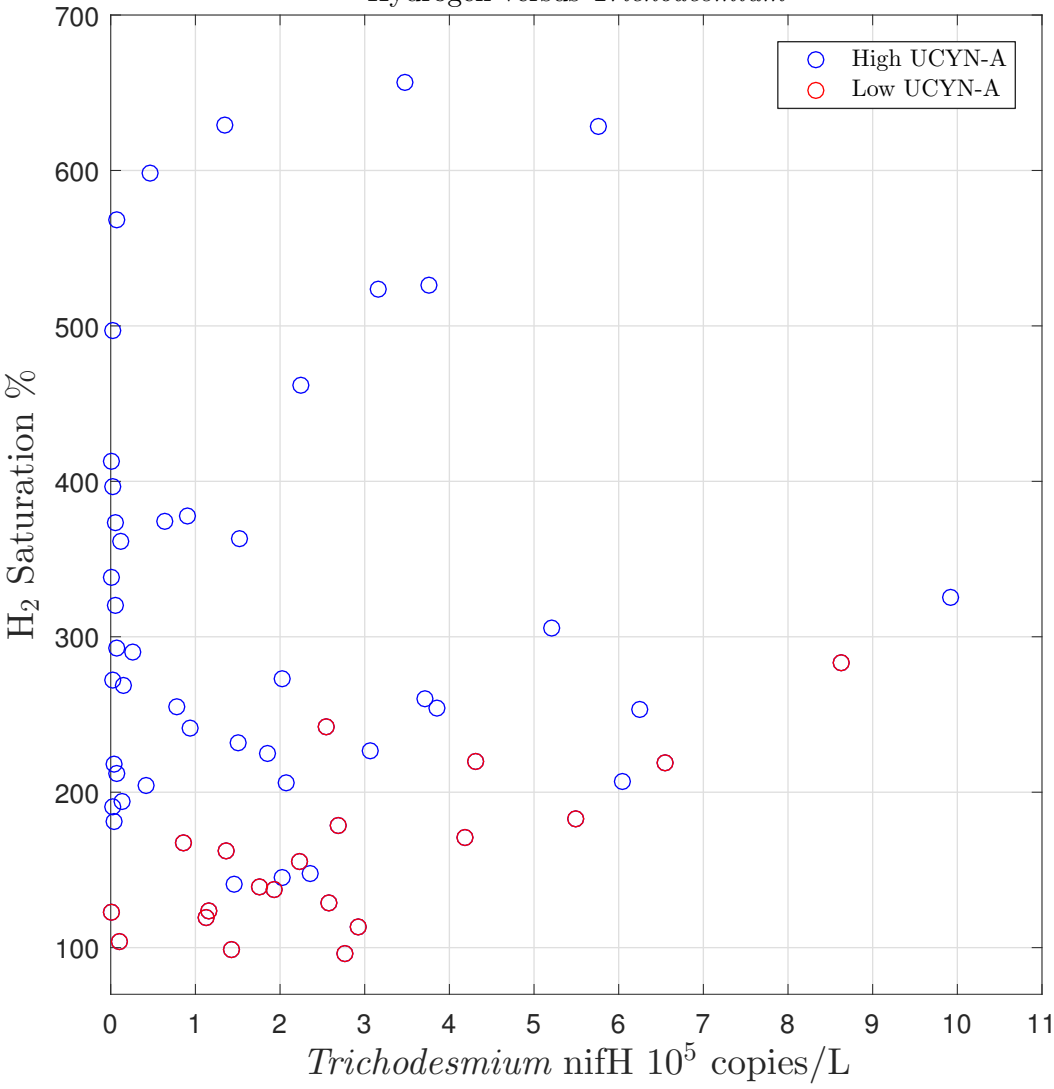
Hydrogen versus *Trichodesmium*

Figure 6.

Observed and Predicted Hydrogen versus Sample Number

